ACTA ABP BIOCHIMICA POLONICA

Vol. 69, No 4/2022
703–710
https://doi.org/10.18388/abp.2020_5809

Regular paper

Long non-coding RNA ERVK13-1 aggravates osteosarcoma through the involvement of microRNA-873-5p/KLF5 axis

Han Xie[1,2], Libing Dai[1], Baoqing Ye[1], Ruixiong Chen[2], Bin Wang[3], Nanwei Zhang[2], Haixiong Miao[1]✉ and Weiguo Liang[1]✉

[1]Department of Orthopedics, Guangzhou Red Cross Hospital Affiliated to Jinan University, Guangzhou, Guangdong 510000, P.R. China; [2]Department of Orthopedics, Huizhou Central People's Hospital, Huizhou, Guangdong 516000, P.R. China; [3]Department of Orthopedics, Huizhou First Hospital, Huizhou, Guangdong 516000, P.R. China

Objective: To explore the effect and mechanism of long noncoding RNA ERVK13-1 on osteosarcoma (OS) cell development by regulation of miR-873-5p/KLF5 axis. Methods: The expression of ERVK13-1 in the collected tissue was detected by RT-qPCR, and then the relationship between ERVK13-1 expression and clinical characteristics of OS patients was analyzed. After OS cell lines were transfected with miR-873-5p inhibitor, si-ERVK13-1, si-KLF5 or their negative controls, the expression of ERVK13-1, miR-873-5p, and KLF5 in OS cell lines were measured, followed by determination of their effects on cell proliferation, migration, and invasion abilities. Moreover, the binding relationships of ERVK13-1 and miR-873-5p, as well as miR-873-5p and KLF5, were verified by the dual-luciferase reporter gene assay. Results: Highly expressed ERVK13-1 was found in OS tissues, which was closely related to tumor size, tumor node metastasis, and distant metastasis. The overall survival of OS patients with high expression of ERVK13-1 was poorer than those with low expression of ERVK13-1. Elevated ERVK13-1 and KLF5 but suppressed miR-873-5p was observed in the OS cell lines U2OS and MG63. Transfection with miR-873-5p inhibitor enhanced the malignant potentials of OS cells, and transfection with si-ERVK13-1 or si-KLF5 reduced these abilities of OS cells. ERVK13-1 bound to miR-873-5p and KLF5 was a target gene of miR-873-5p. Conclusion: The ERVK13-1/miR-873-5p/KLF5 axis confers vital effect on the occurrence and progression of OS, thus providing possible guidance for the clinical treatment of OS.

Keywords: osteosarcoma, ERVK13-1, microRNA-873-5p, KLF5, proliferation, migration, invasion, long non-coding RNA

Received: 03 August, 2021; revised: 06 December, 2021; accepted: 24 January, 2022; available on-line: 22 October, 2022

✉e-mail: liangweiguo1961@126.com (WL); miaohaixiong@163.com (XM)

Acknowledgements of Financial Support: This research was funded by the grants from Guangdong Provincial Medical Scientific Research Project (Grant No. A2017501) and Guangzhou Medical and Health Technology General Guidance Project (Grant No. 20171A011252; 20161A011017).

Abbreviations: ceRNAs, competitive endogenous RNAs; KLF5, Krüppel-like factor 5; lncRNA, long non-coding RNA; mRNAs, messenger RNAs; miRNAs, MicroRNAs; OS, osteosarcoma

INTRODUCTION

Osteosarcoma (OS), an osteoid-producing malignancy of mesenchymal origins, is characterized by deposition of immature osteoid matrix by spindle cells of mesenchymal origin and frequently occurs in children and adolescents (Lamoureux *et al.*, 2007, Durfee *et al.*, 2016, Lindsey *et al.*, 2017). Specifically, OS can be seen in the bones of the lower extremities and humerus of young patients (Serra & Hattinger, 2017). Although surgical resection of the primary lesion and systemic preoperative and postoperative multidrug chemo-therapy have been widely employed for OS treatment, the prognosis is still unsatisfactory with estimated 5-year survival rate of only 65~70% (Serra & Hattinger, 2017; Yao *et al.*, 2020). Therefore, a new perspective is warranted to improve their prognosis and survival rate.

Long non-coding RNA (lncRNA) is a type of oligonucleotide with a length of more than 200 nt without protein-coding potentials (Wang *et al.*, 2020). The regulatory role of lncRNAs in the progression of human cancers has been gradually revealed. For example, lncRNA PVT1 is responsible for propagation and invasion of colorectal cancer cells by the upregulation of miR-214-3p (Shang *et al.*, 2019). Additionally, the abnormally expressed lncRNAs have been found in OS and proved to correlate with the prognosis (Yan *et al.*, 2018, Huang *et al.*, 2020). Important role of ERVK13-1 in heart failure has been found (Han, 2019), however, its function in OS initiation and progression remains unclear.

MicroRNAs (miRNAs) are a subclass of small non-coding transcripts with 20~22 nucleotides, and their potential roles in tumorigenesis through regulation of oncogenes or tumor-suppressor genes has been discovered (Ren *et al.*, 2020). A previous document has clarified a reduction in miR-873 expression in OS tissues and cell lines, and miR-873 overexpression leads to repress the malignant properties of OS cells (Liu *et al.*, 2019). Accumulating evidence has highlighted the function of competitive endogenous RNAs (ceRNAs) to regulate cancer development by sponging miRNAs and targeting messenger RNAs (mRNAs) (Zhao *et al.*, 2020). The miR-873-5p/ZEB2 axis confers a vital effect on HOTAIRM1-influenced proliferation and apoptosis of glioma cells (Lin *et al.*, 2020). However, whether the anticancer functions mediated by miR-873-5p in OS are related to ERVK13-1 remains to be studied.

Krüppel-like factor 5 (KLF5), as a zinc-finger transcription factor, possesses various functions in eukaryotic cells, such as regulation of proliferation, migration, and differentiation (Huang *et al.*, 2020). Importantly, KLF5 exerts a crucial effect on the biological behavior of OS cells (Cai *et al.*, 2018). Exploring the interaction of lncRNA-miRNA-mRNA may be helpful to understand the mechanism and pathogenesis of cancers. Therefore, in this study, we tried to explore the regulatory roles of ERVK13-1, miR-873-5p, and KLF5 in OS development.

MATERIALS AND METHODS

Ethical statement

The study was conducted according to the Declaration of Helsinki. The study protocol concerning humans was approved by the Ethics Committee of Huizhou Central People's Hospital (LLBA201809A). All the patients provided their written informed consent.

Subjects

A total of 20 OS patients who did not receive radiation or chemotherapy were recruited from Huizhou Central People's Hospital. After surgical resection, OS tissues and para-carcinoma tissues were collected and stored in liquid nitrogen for subsequent RNA or protein extraction.

Cell culture

Human OS cell lines U2OS and MG63 as well as human fetal osteoblast cell line hFOB1.19 were supplied by the Cell Resource Center of Shanghai Institutes for Biological Sciences, Chinese Academy of Sciences. All cell lines were incubated in Dulbecco's modified eagle medium (DMEM, Gibco, Grand Island, NY, USA) with 10% fetal calf serum (FBS), 1% penicillin and 1% streptomycin under 5% CO_2 at 37°C.

Cell transfection and grouping

U2OS and MG63 cells were transfected with 30 nM miR-873-5p inhibitor, 2 μg si-ERVK13-1, 2 μg si-KLF5 (GenePharma, Shanghai, China) or their negative controls, respectively by utilizing the LipoFiter™ reagent (Hanbio, Shanghai, China). Three replicates were set for the transfection procedure. Inhibitor is for miRNA inhibition, which can effectively inhibit the function of endogenous mature miRNA, thereby inhibiting the expression of miRNA. siRNA is an important effector molecule on which RNA interference occurs, and it can interfere the expression of target genes. The detailed grouping was seen as follows: Blank group (without any transfection), inhibitor NC group (U2OS and MG63 cells were transfected with NC of miR-873-5p inhibitor), inhibitor group (U2OS and MG63 cells were transfected with miR-873-5p inhibitor), si-NC group (U2OS and MG63 cells were transfected with NC of si-ERVK13-1 or si-KLF5), si-ERVK13-1 group (U2OS and MG63 cells were transfected with silenced ERVK13-1), si-KLF5 group (U2OS and MG63 cells were transfected with silenced KLF5), inhibitor-miR-873-5p + si-ERVK13-1 group (U2OS and MG63 cells were transfected with miR-873-5p inhibitor and silenced ERVK13-1). The subsequent experiment was implemented after 24 h of transfection.

Reverse transcription quantitative polymerase chain reaction (RT-qPCR)

The total RNA was extracted from U2OS, MG63, and hFOB1.19 cells, respectively, employing TRIzol (Invitrogen, Carlsbad, CA, USA). The concentration and purity of RNA were inspected. Reverse transcription was carried out utilizing the reverse transcription kit (TaKaRa, Tokyo, Japan) according to the instructions of the kit and random primers. Light Cycler 480 (Roche, Indianapolis, IN, USA) fluorescent quantitative PCR instrument was employed to quantitate gene expression. The reaction conditions were set in accordance with the instructions of the fluorescent quantitative PCR kit (SYBR Green Mix, Roche Diagnostics, Indianapolis, IN). Following a 5 min pre-degeneration step at 95°C, RNAs underwent 40 cycles consisting of a 10 s denaturing procedure at 95°C, a 10 s annealing step at 60°C and a 20 s extension at 72°C. Each reaction possesses 3 replicates. U6 was selected as an internal reference of miRNA, and glyceraldehyde-3-phosphate dehydrogenase (GAPDH) was regarded as the internal reference of mRNA and lncRNA. The $2^{-\Delta\Delta Ct}$ method was used for data analysis. The amplified primer sequence of each gene and its internal reference gene are exhibited in Table 1.

Table 1. Primer sequences

Name of primer	Sequences
U6-F	CTCGCTTCGGCAGCACA
U6-R	ACGCTTCACGAATTTGCGT
Hsa-miR-873-5p-F	GCAGGAACTTGTGAGTCTCCT
Hsa-miR-873-5p-R	CTCTACAGCTATATTGCCAGCCAC
GAPDH-F	AATGGGCAGCCGTTAGGAAA
GAPDH-R	GCGCCCAATACGACCAAATC
ERVK13-1-F	ATGCCGTGTTTCCTGTCTGT
ERVK13-1-R	TGCAAACCCACTTGAACCCT
KLF5-F	ACGCTTGGCCTATAACTTGG
KLF5-R	ACTGGTCTACGACTGAGGCA

Notes: F: forward primer; R: reversed primer.

Western blot

Cells were lysed with RIPA (Beyotime, Shanghai, Beijing) and centrifuged to obtain protein sample. The protein concentration was determined by BCA kit (Beyotime), and the corresponding volume of protein was mixed with the loading buffer (Beyotime) followed by 3 min of denaturation in a boiling-water bath. Then, the protein was separated by prepared 10% sodium dodecyl sulfate-polyacrylamide gel electrophoresis (SDS/PAGE) at 80 V. When bromophenol blue entered the separation gel, the electrophoresis was conducted to 120 V for 1–2 h. After that, proteins were transferred to membranes at 300 mA for 60 min in ice-bath. The membranes were rinsed 1 ~ 2 min with washing solution and then sealed in the blocking solution at room temperature for 60 min or sealed overnight at 4°C. Then the membranes were incubated with the primary antibodies: rabbit anti-human GAPDH (5174S, 1:1000, Cell Signaling, Boston, USA) and KLF5 (ab24331, 1:1000, Cell Signaling, Boston, USA) at room temperature in a shaking table for 1 h. Afterwards, the membranes were washed with washing solution 3 times (each for 10 min) and then incubated with the secondary antibody against goat anti-rabbit IgG (1:5000, Beijing ComWin Biotech Co., Ltd., Beijing, China) labeled with horseradish peroxidase for 1 h at room temperature. After washing, the membranes underwent X-ray film exposure and development.

Dual-luciferase reporter gene assay

The prediction for the binding site of miR-873-5p and ERVK13-1 was performed by using the online database StarBase (https://starbase.sysu.edu.cn/index.php). Addition-

ally, the online software PITA (https://genie.weizmann.ac.il/pubs/mir07/mir07_data.html) was applied to predict the binding region of miR-873-5p and KLF5. The mutated type sequences and wild type sequences (mut-ERVK13-1, wt-ERVK13-1, mut-KLF5 and wt-KLF5) were designed and synthesized in accordance with the predicted results and cloned into luciferase reporter gene vector (pGL3-Promoter, Promega, MADISON, WI, USA). Then the vectors were co-transfected with miR-873-5p mimic or mimic-NC (30 nM, GenePharma), respectively, into HEK293T cells. After transfection, the fluorescence intensity of cells in each group was measured by the dual-luciferase reporter gene assay kit (Promega, Madison, WI, USA) to determine the binding of miR-873-5p to ERVK13-1 and miR-873-5p to KLF5. Cells were grouped into mimic + mut-ERVK13-1 group, mimic + wt-ERVK13-1 group, mimic NC + mut-ERVK13-1 group, mimic NC + wt-ERVK13-1, mimic + mut-KLF5 group, mimic + wt-KLF5 group, mimic NC + mut-KLF5 group and mimic NC + wt-KLF5 group. This experiment was repeated 3 times.

Cell counting kit-8 (CCK-8) assay

After transfection, 100 μL suspension of U2OS and MG63 cells were seeded into 96-well plates (1×10^5 cells/ml). The experiment was designed with three replicates. Following 12, 24, 36, and 48 h of incubation, cells in each well were exposed to 10 μl of CCK-8 reagent for 3 h of incubation. Absorbance was detected at 450 nm wavelength.

Colony formation assay

Following transfection, cells in the logarithmic phase were triturated thoroughly. Cell suspension was diluted to a concentration of 200 cells/well and cultured for 2 weeks under 5% CO_2 at 37°C. The culture medium was replaced duly according to the pH value during incubation. Cell culture was stopped when colonies were visible. After removal of medium, cells were fixed in methanol for 15 min followed by 10 min of Giemsa staining. Cells were then washed with running water, air dried and counted. Three replicates were set for this assay.

Transwell assay

Transwell chamber (pore size: 8 μm, Corning, New York, USA) covered with Matrigel was used for cell invasion detection. About 0.5 mL of serum-free culture medium was added to the chamber for incubation at 37°C, 5% CO_2 for 2 h. Then, culture medium was removed. Cells in the logarithmic phase were made into single-cell suspension and uniformly inoculated in the six-well plate for incubation at 37°C in 5% CO_2. Three duplicates were set for each well. Upon reaching 70% ~ 90% confluency, cells were subjected to different treatment and then cultured at 37°C in 5% CO_2 for 24 h, followed by digestion and collection. Then, cells were resuspended in serum-free DMEM with cell concentration adjusted. About 600 μL culture medium containing 10% FBS was pipetted into basolateral chamber, and 100 μL cell suspension was aspirated into apical chamber. After incubation for 24 h, the non-invaded cells on the apical chamber of the membrane were removed with a cotton swab. The invaded cells were fixed in 4% paraformaldehyde for 20 min and subjected to Wright-Giemsa staining. Five fields were selected randomly under a high-power lens to count invaded cells and capture pictures.

Cell scratch assay

Cells in the logarithmic phase were collected and prepared into a single-cell suspension (5×10^5 cells/ml), which was uniformly inoculated on a six-well plate. After 24 h, the treated cells were cultured in an incubator at 37°C with 5% CO_2. Then, cells were scratched using a 100 μL sterile pipette tip which was as perpendicular to cells as possible to ensure that the scratch width of each group was basically the same. PBS was employed to wash cells twice to remove the scratched cells. Then cells were cultured with serum-free DMEM. Photographs were captured and the cell migration rate was calculated based on the changes in scratch distance. Cell migration rate = (scratch width at 0 h- scratch width after 24 h)/scratch width at 0 h×100%.

Statistical analysis

Data were analyzed employing GraphPad Prism 7.0 and showed as mean ± standard deviation (S.D.). The overall survival rate was displayed by the Kaplan-Meier method and the difference between the curves was analyzed by the log-rank test. χ^2test (chi-square test) was utilized to evaluate the relationship between ERVK13-1 expression and clinicopathological characteristics of OS patients. Statistical comparisons between two groups were made using *T* test. The one-way analysis of variance was adopted followed by Tukey's multiple comparison tests for comparisons among more than two groups. Significance was set at $P<0.05$.

RESULTS

ERVK13-1 is highly expressed in OS and correlated with adverse clinical outcomes of OS patients

To inspect the role of ERVK13-1 in OS, RT-qPCR was applied to assess the level of ERVK13-1 in 20 cases

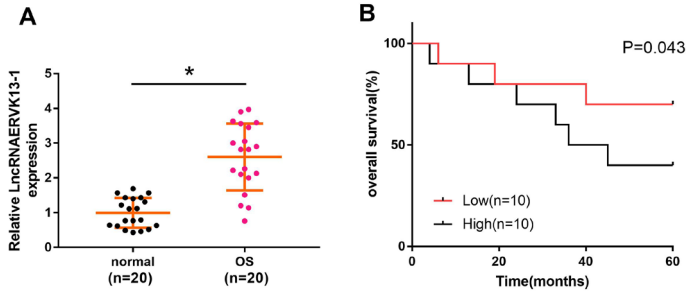

Figure 1. Highly expressed ERVK13-1 in OS tissues is correlated with OS progression
Note: The expression of ERVK13-1 in OS tissues and para-carcinoma tissues were detected by RT-qPCR (A), and Kaplan-Meier survival curve was exhibited (B); *$P<0.05$; OS, osteosarcoma.

Table 2. Relationship between the ERVK13-1 expression and clinical characteristics of 20 patients with OS

Clinical characteristic	ERVK13-1		*P*-value
	High expression	Low expression	
Age (years)			0.628
< 18	8	6	
≥ 18	2	4	
Sex			0.141
Male	5	1	
Female	5	9	
Tumor size (cm)			0.019
< 5	3	9	
> 5	7	1	
TNM stage			0.023
I or II	2	8	
III or IV	8	2	
Distant metastasis			0.046
Presence	6	1	
Absence	4	9	

Notes: OS, osteosarcoma; TNM, tumor node metastasis.

of OS tissues and para-carcinoma normal tissues. The results presented highly expressed ERVK13-1 in tissues obtained from OS patients than in normal tissues (Fig. 1A, $^{*}P<0.05$). Then, 20 patients with OS were divided into two groups based on the median (exact value: 2.65) of ERVK13-1 expression: low expression group (n=10) and high expression group (n=10). As depicted in Table 2, high level of ERVK13-1 was obviously related to tumor size ($P=0.019$), tumor node metastasis stage ($P=0.023$), and distant metastasis ($P=0.046$). Additionally, the overall survival of patients in the high expression group was shorter than those in the low expression group (Fig. 1B, $P=0.043$). These data illustrated close correlation between ERVK13-1 expression and the progression of OS.

Upregulated ERVK13-1 and downregulated miR-873-5p were seen in OS cells

We then found elevated ERVK13-1 expression and reduced miR-873-5p expression in human OS cell lines U2OS and MG63 relative to human fetal osteoblast hFOB1.19 cells (Fig. 2A, B, $^{**}P<0.01$). Transfection with si-ERVK13-1 contributed to suppressed ERVK13-1 expression (Fig. 2C–D, $^{**}P<0.01$) and elevated miR-873-5p expression (Fig. 2E–F, $^{*}P<0.05$) in OS cell lines. Transfection with miR-873-5p inhibitor suppressed miR-873-5p expression (Fig. 2E–F, $^{*}P<0.05$) and its expression was increased by treatment of si-ERVK13-1 and miR-873-5p inhibitor than by miR-873-5p inhibitor treatment alone (Fig. 2E–F, $^{*}P<0.05$). No obvious change in expression of miR-873-5p was noticed in the inhibitor NC, si-NC, and inhibitor-miR-873-5p + si-ERVK13-1 groups (Fig. 2E–F). The above results indicated that ERVK13-1 negatively regulated the expression of miR-873-5p.

ERVK13-1 maintains biological behavior of OS cells by negatively mediating miR-873-5p

Results of CCK-8 implied the restrained cell viability in U2OS and MG63 cells after transfection with si-ERVK13-1, and enhanced proliferation ability in the cells transfected with miR-873-5p inhibitor (Fig. 3A–B, $^{*}P<0.05$). Compared with the si-ERVK13-1 group, the inhibitor-miR-873-5p + si-ERVK13-1 group possessed potentiated cell viability. There was no obvious difference in proliferation rate in inhibitor NC, si-NC, and inhibitor-miR-873-5p + si-ERVK13-1 groups. Similar findings were obtained from colony formation assay, which suggested the crucial effects of ERVK13-1 and miR-873-5p on OS cell proliferation (Fig. 3C). Transwell and cell scratch assays highlighted that the silencing of ERVK13-1 led to diminished abilities of cell invasion and migration, and knockdown of miR-873-5p contributed to the contrary findings (Fig. 3D–E, $^{*}P<0.05$). Moreover, the co-treatment of si-ERVK13-1 and miR-873-5p inhibitor brought about more significant enhancement than si-ERVK13-1 treatment alone (Fig. 3D–E, $^{*}P<0.05$). These findings indicated that downregulation of ERVK13-1 was capable of inhibiting the proliferation, invasion, and migration abilities of OS cells, while suppression of miR-873-5p promoted these properties of OS cells. ERVK13-1 was found to facilitate the proliferation, invasion, and migration of OS cells by the negative regulation of miR-873-5p expression.

Highly expressed KLF5 in OS cells

Analyses of RT-qPCR and Western blot yielded that the mRNA and protein expression levels of KLF5 in OS cell lines U2OS and MG63 were significantly higher than those of hFOB1.19 cells (Fig. 4A–B, $^{*}P<0.05$). Transfection of si-ERVK13-1 led to repressed KLF5 level (*vs.* the si-NC group); while miR-873-5p inhibitor treatment possessed heightened KLF5 expression (*vs.* the inhibitor NC group); and cells in the inhibitor-miR-873-5p + si-ERVK13-1 group had enhanced mRNA and protein levels of KLF5 (Fig. 4C–F, $^{*}P<0.05$, *vs.* the si-ERVK13-1 group). No significant difference in KLF5 expression was obtained from the inhibitor NC, si-NC,

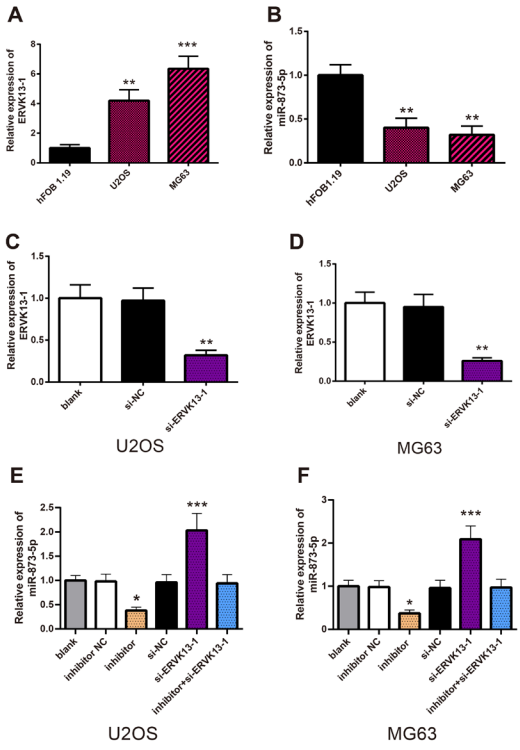

Figure 2. ERVK13-1 was up-regulated while miR-873-5p expression was down-regulated in OS cell lines
Notes: RT-qPCR was applied to evaluate the expression of ERVK13-1 (**A**) and miR-873-5p (**B**) in hFOB1.19, U2OS and MG63 cells; $^{*}P<0.05$, $^{**}P<0.01$, $^{***}P<0.001$, compared to hFOB1.19 cells. After transfection with si-ERVK13-1, ERVK13-1 expression in U2OS cells (**C**) and MG63 (**D**) cells was assessed by RT-qPCR. Additionally, RT-qPCR was applied to detect miR-873-5p level in OS cells (**E–F**) after different transfection; $^{*}P<0.05$, $^{***}P<0.001$, compared to compared to si-NC group or inhibitor NC group. Blank group (without any transfection), inhibitor NC group (cells were transfected with the negative control of miR-873-5p inhibitor), inhibitor group (cells were transfected with miR-873-5p inhibitor), si-NC group (cells were transfected with the negative control of si-ERVK13-1), si-ERVK13-1 group (cells were transfected with si-ERVK13-1), inhibitor-miR-873-5p + si-ERVK13-1 group (U2OS and MG63 cells were transfected with miR-873-5p inhibitor and si-ERVK13-1).

and inhibitor-miR-873-5p + si-ERVK13-1 groups. Taken these data together, miR-873-5p negatively regulated the expression of KLF5.

KLF5 was able to induce the proliferation, invasion, and migration of OS cells

The notably reduced KLF5 in OS cell lines transfected with si-KLF5 was evaluated by Western blot (Fig. 5A, $^{**}P<0.01$). Findings obtained from CCK-8 ($^{*}P<0.05$), colony formation assay ($^{**}P<0.01$), transwell and cell scratch assays ($^{**}P<0.01$) revealed that transfection with si-KLF5 restrained abilities of cell proliferation, invasion, and migration (Fig. 5B–E). The above results implied that the KLF5 downregulation could hinder the OS cell proliferation, invasion, and migration. Additionally, KLF5 conferred a carcinogenic role in OS.

ERVK13-1 negatively regulated miR-873-5p and miR-873-5p targeted KLF5

As depicted in Fig. 6A, the binding site of miR-873-5p and ERVK13-1 in the 3'UTR region was predicted by starBase. Then, mut-ERVK13-1 and wt-ERVK13-1 were accordingly designed for dual-luciferase reporter gene as-

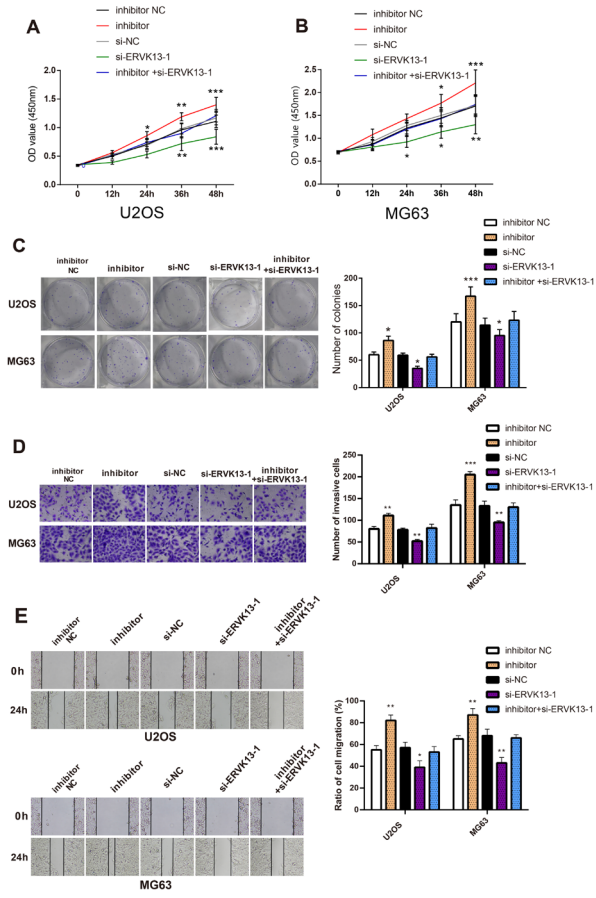

Figure 3. ERVK13-1 induces OS cell malignant potentials through regulation of miR-873-5p
Notes: After transfection, the OD values of U2OS cells (**A**) and MG63 cells (**B**) at different culture times were measured by CCK-8. Colony formation assay was utilized for inspection of proliferation ability of OS cells (**C**), transwell for assessment of cell invasion ability (**D**) and cell scratch assay for examination of cell migration ability (**E**); $^{*}P<0.05$, $^{**}P<0.01$, $^{***}P<0.001$, compared to si-NC group or inhibitor NC group; OD, optical density; OS, osteosarcoma. Inhibitor NC group (cells were transfected with the negative control of miR-873-5p inhibitor), inhibitor group (cells were transfected with miR-873-5p inhibitor), si-NC group (cells were transfected with the negative control of si-ERVK13-1), si-ERVK13-1 group (cells were transfected with si-ERVK13-1), inhibitor-miR-873-5p + si-ERVK13-1 group (cells were transfected with miR-873-5p inhibitor and si-ERVK13-1).

say. We found that HEK-293T cells co-transfected with wt-ERVK13-1 and miR-873-5p mimic had relatively lower luciferase activity than cells co-transfected with wt-ERVK13-1 and mimic NC (Fig. 6C, $^{*}P<0.05$). The relative luciferase activity in the mimic + mut-ERVK13-1 group was not statistically different from the mimic NC + mut-ERVK13-1 and mimic NC + wt-ERVK13-1 groups.

The binding site of miR-873-5p and KLF5 was predicted by the online software PITA (Fig. 6B), and the mut-KLF5 and wt-KLF5 were subsequently constructed. Results of dual-luciferase reporter gene assay revealed that the relative luciferase activity in cells co-transfected with wt-KLF5 and miR-873-5p mimic was lower than cells co-transfected with wt-KLF5 and mimic NC (Fig. 6D, $^{*}P<0.05$). There was no marked difference in the mimic + mut-KLF5, mimic NC + mut-KLF5, and mimic NC + wt-KLF5 groups. The above results con-

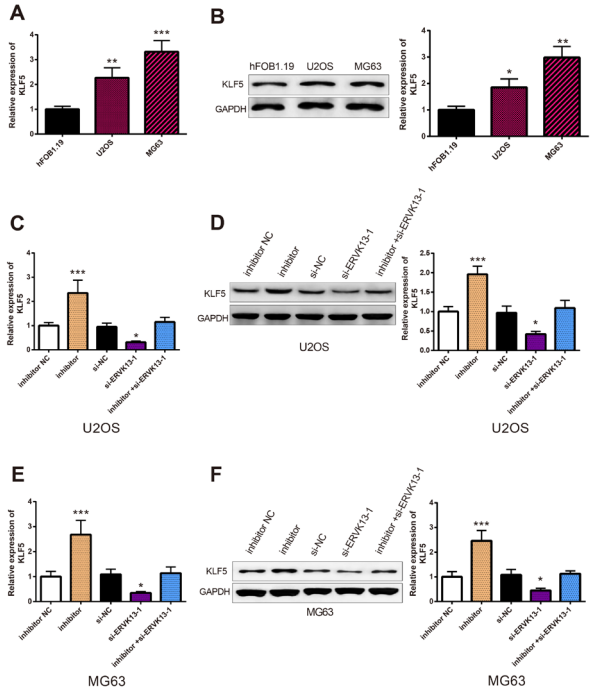

Figure 4. KLF5 is negatively correlated with miR-873-5p and positively correlated with ERVK13-1
Notes: RT-qPCR (**A**) and Western blot (**B**) were employed to examine KLF5 level in U2OS, MG63 and hFOB1.19 cells; $^{*}P<0.05$, $^{**}P<0.01$, $^{***}P<0.001$, compared to hFOB1.19 cells. After transfection, the mRNA and protein expression of KLF5 in U2OS (**C–D**) and MG63 cells (E-F) were detected by RT-qPCR and Western blot; $^{*}P<0.05$, $^{***}P<0.001$, compared to si-NC group or inhibitor NC group. Inhibitor NC group (cells were transfected with the negative control of miR-873-5p inhibitor), inhibitor group (cells were transfected with miR-873-5p inhibitor), si-NC group (cells were transfected with the negative control of si-ERVK13-1), si-ERVK13-1 group (cells were transfected with si-ERVK13-1), inhibitor-miR-873-5p + si-ERVK13-1 group (U2OS and MG63 cells were transfected with miR-873-5p inhibitor and si-ERVK13-1).

cluded that both ERVK13-1 and KLF5 could bind to miR-873-5p. Therefore, ERVK13-1 was considered to upregulate KLF5 by negative mediation of miR-873-5p, thereby promoting the proliferation, invasion, and migration of OS cells.

DISCUSSION

OS is a relatively rare bones tumor with incidence of 3.4 cases per million people each year in the world (Misaghi *et al.*, 2018). Nevertheless, little prognostic improvement in OS has been generated from the last 20 years of research and a new perspective is still warranted. Here we focused on ERVK13-1 and its mechanism in OS. We further pursued the understanding of the molecular mechanism along the ceRNA direction. By means of target prediction, we found that ERVK13-1 competitively bound to miR-873-5p, and KLF5 was verified as a target gene of miR-873-5p. Thereby, we hypothesized that the ERVK13-1/miR-873-5p/KLF5 axis could regulate the progression of OS. Through verification using a series of cell experiments, we observed that ERVK13-1 was engaged in the proliferation, migration, and invasion of OS cells through working as a ceRNA to sponge miR-873-5p. More evidence from this study suggested that ERVK13-1 aggravated OS by sponging miR-873-5p to modulate KLF5 expression.

Initially, highly expressed ERVK13-1 was also found in OS tissues. Meanwhile, positive association was found between the high expression of ERVK13-1 and the development of tumor size, distant metastasis, and tumor node metastasis stage and negatively related to the overall survival of OS patients. In addition, we observed that ERVK13-1 expression was significantly higher in OS cell lines U2OS and MG63 than in human fetal osteoblast hFOB1.19 cells. Numerous studies have exhibited that the aberrant expression of lncRNAs is related to the OS development and metastasis. For example, lncRNA DANCR regulates migration and invasion of OS cells by targeting the miR-149/MSI2 axis (Zhang *et al.*, 2020). LINC00319 can promote progression of OS by the miR-455-3p/NFIB axis mediation (Sun *et al.*, 2020). In the current study, ERVK13-1, a newly identified and rarely researched lncRNA, was speculated to be involved in the development of OS. Subsequently, CCK-8, colony formation assay, transwell and cell scratch assays were utilized to analyze OS cell abilities of proliferation, invasion, and migration. We discovered that reduced ERVK13-1 suppressed OS development, as evidenced by diminished cell viability, reduced invasion capacity, and weakened migration ability in OS cell lines

MiR-873-5p plays a tumor-suppressive role in various malignancies, such as papillary thyroid cancer and colorectal cancer (Wang *et al.*, 2019; Wang *et al.*, 2020). Here, RT-qPCR further verified the decrease of miR-873-5p expression in OS cell lines, which was in line with previous research (Zhang *et al.*, 2020). Apart from this finding, the bioinformatic analysis and dual-luciferase reporter gene assay described that miR-873-5p was confirmed as a target of ERVK13-1. Transfection with miR-873-5p inhibitor inhibited the mRNA level of miR-873-5p, whereas the following silencing of ERVK13-1 reversed this trend, implying that ERVK13-1 could repress miR-873-5p expression by acting as an endogenous sponge. LncRNAs are ceRNAs containing miRNA response elements, which can inhibit miRNAs on downstream genes by competitively binding miRNA sites (Ma *et al.*, 2020). This finding triggers us to explore whether miR-873-5p can also elicit a significant effect on OS progression through a similar regulatory mechanism. For verification purpose, the expressions of miR-873-5p and ERVK13-1 were incapacitated in OS cell lines. We found that ERVK13-1 knockdown caused repressed biological behaviors of OS cells; miR-873-5p suppression induced enhanced OS cell proliferation, migration, and invasion abilities. Therefore, we concluded that ERVK13-1 could maintain the biological function of OS cells by sponging miR-873-5p. Such mechanism has been also confirmed in the former study. In non-small cell lung cancer, lncRNA TDRG1 can induce the metastasis of cancer cells through regulating the miR-873-5p/ZEB1 axis (Hu *et al.*, 2019).

To further expound the mechanism of ERVK13-1-miR-873-5p on governing of OS progression, the dual-luciferase reporter gene assay was employed to seek after the potential target genes of miR-873-5p. Our results supported that KLF5 was the putative target of miR-873-5p in OS cell lines. KLF5, a zinc-finger transcription factor, has various functions in different cellular processes, including proliferation and invasion (Ma *et al.*, 2017, Ma *et al.*, 2020). The abnormally expressed KLF5 is related to a variety of human diseases and cancers (Pattison *et al.*, 2016). Previous work proposed that KLF5 participates in miR-493-5p-inhibited OS cell pro-

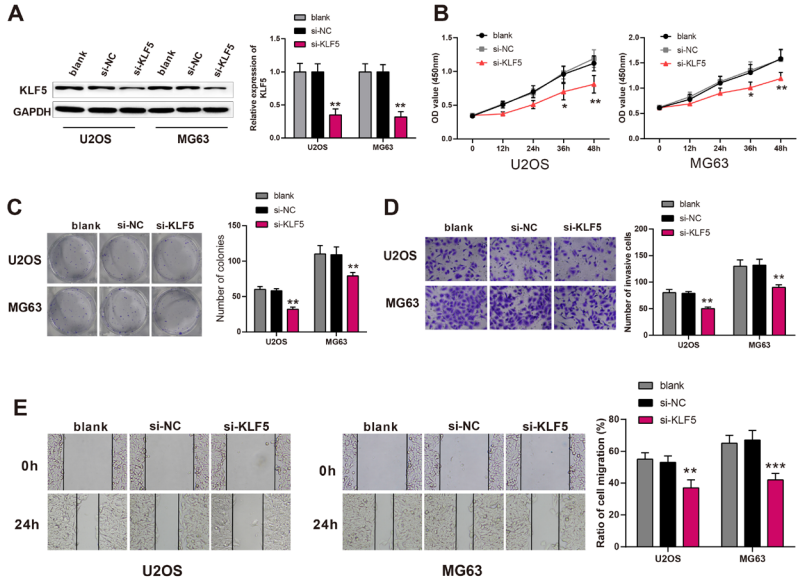

Figure 5. KLF5 induces OS proliferation, migration, and invasion
Notes: Western blot was applied to detect the expression of KLF5 in OS cells (**A**). After transfection, the OD values of OS cells at different culture times were performed by CCK-8 (**B**). The proliferation of OS cells was detected by colony formation assay (**C**). Transwell was adopted to measure the invasion ability of U2OS and MG63 cells (**D**). Migration ability of OS cells was determined by cell scratch assay (**E**); $^{*}P<0.05$, $^{**}P<0.01$, $^{***}P<0.001$, compared to si-NC group; OD, optical density; OS, osteosarcoma. Blank group (without any transfection), si-NC group (cells were transfected with the negative control of si-KLF5), si-ERVK13-1 group (cells were transfected with si-ERVK13-1), si-KLF5 group (cells were transfected with si-KLF5).

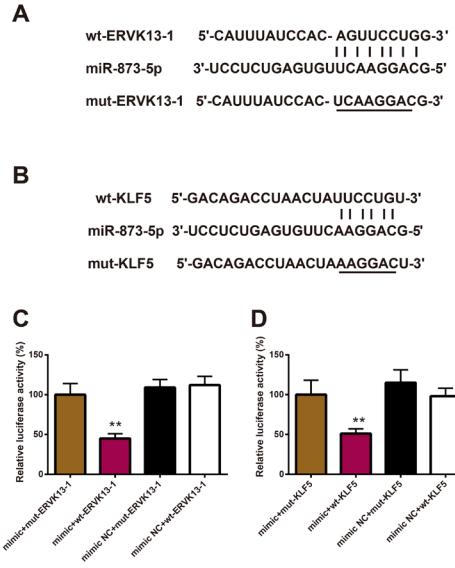

Figure 6. ERVK13-1 negatively regulates miR-873-5p, and miR-873-5p negatively regulates KLF5
Notes: The binding sites of miR-873-5p and ERVK13-1 as well as miR-873-5p and KLF5 in the 3′-UTR region were respectively predicted by Starbase (**A**) and PITA (**B**). Dual-luciferase reporter gene assay confirmed the interaction of ERVK13-1 and miR-873-5p (**C**); $^{**}P<0.01$, compared to mimic + mut-ERVK13-1 group. Dual-luciferase reporter gene assay verified the interaction between KLF5 and miR-873-5p (**D**); $^{**}P<0.01$, compared to mimic + mut-KLF5 group. mimic + mut-ERVK13-1 group (The mutation sequence of ERVK13-1 was inserted into pGL3-Basic and co-transfected with miR-873-5p mimic into HEK239T cells), mimic + wt-ERVK13-1 group (The wild type sequence of ERVK13-1 was inserted into pGL3-Basic and co-transfected with miR-873-5p mimic into HEK239T cells), mimic NC + mut-ERVK13-1 group (The mutation sequence of ERVK13-1 was inserted into pGL3-Basic and co-transfected with NC of miR-873-5p mimic into HEK239T cells), mimic NC + wt-ERVK13-1 group (The wild type sequence of ERVK13-1 was inserted into pGL3-Basic and co-transfected with NC of miR-873-5p mimic into HEK239T cells), mimic + mut-KLF5 group (The mutation sequence of KLF5 was inserted into pGL3-Basic and co-transfected with miR-873-5p mimic into HEK239T cells), mimic + wt-KLF5 group (The wild type sequence of KLF5 was inserted into pGL3-Basic and co-transfected with miR-873-5p mimic into HEK239T cells), mimic NC + mut-KLF5 group (The mutation sequence of KLF5 was inserted into pGL3-Basic and co-transfected with NC of miR-873-5p mimic into HEK239T cells) and mimic NC + wt-KLF5 group (The wild type sequence of KLF5 was inserted into pGL3-Basic and co-transfected with NC of miR-873-5p mimic into HEK239T cells).

liferation and invasion (Cai *et al.*, 2018). Our study identified that KLF5 conferred a carcinogenic effect on OS to induce OS cell proliferation, invasion, and migration. Collectively, ERVK13-1 could indeed sponge miR-873-5p to regulate KLF5 expression, thus modulating the progression of OS.

To conclude, our data demonstrated that the ERVK13-1/miR-873-5p/KLF5 axis was a novel signal that regulated OS development and progression. These findings provided a rationale for the development of alternative strategies for the clinical treatment of OS. However, more regulatory networks of ERVK13-1 in human cancer require further elucidation for the multi-layered complexity of ceRNA crosstalk and competition. Additionally, the clinical applications await deeper investigation, such as in vivo experiments to draw a comprehensive picture of the potential molecular mechanisms of ERVK13-1 in OS.

Declarations

Acknowledgement. Not applicable.

Declare of interests. The author declares they have no competing interests.

Ethical approval. The study was conducted according to the Declaration of Helsinki. The study protocol concerning human was approved by the Ethics Committee of Huizhou Central People's Hospital (LLBA201809A). All the patients provided their written informed consent.

Statement of Informed Consent. Not applicable.

Authors' contributions. LWG; MHX and XH conceived the ideas. LWG; MHX and XH designed the experiments. DLB; YBQ and CRX performed the experiments. CRX; WB and ZNW analyzed the data. LWG and MHX provided critical materials. XH and YBQ wrote the manuscript. LWG and MHX supervised the study. All the authors have read and approved the final version for publication.

Availability of data and materials. The datasets used or analyzed during the current study are available from the corresponding author on reasonable request.

REFERENCE

Cai W, Xu Y, Yin J, Zuo W, Su Z (2018) miR5905p suppresses osteosarcoma cell proliferation and invasion *via* targeting KLF5. *Mol Med Rep* **18**: 2328–2334. https://doi.org/10.3892/mmr.2018.9173

Durfee RA, Mohammed M, Luu HH (2016) Review of osteosarcoma and current management. *Rheumatol Ther* **3**: 221–243. https://doi.org/10.1007/s40744-016-0046-y

Han DM (2019) Sub-pathway based approach to systematically track candidate sub-pathway biomarkers for heart failure. *Exp Ther Med* **17**: 3162–3168. https://doi.org/10.3892/etm.2019.7319

Hu X, Mu Y, Wang J, Zhao Y (2019) LncRNA TDRG1 promotes the metastasis of NSCLC cell through regulating miR-873-5p/ZEB1 axis. *J Cell Biochem*. Epub ahead of print. https://doi.org/10.1002/jcb.29559

Huang H, Han Y, Chen Z, Pan X, Yuan P, Zhao X, Zhu H, Wang J, Sun X, Shi P (2020) ML264 inhibits osteosarcoma growth and metastasis *via* inhibition of JAK2/STAT3 and WNT/beta-catenin signalling pathways. *J Cell Mol Med* **24**: 5652–5664. https://doi.org/10.1111/jcmm.15226

Huang Y, Xu YQ, Feng SY, Zhang X, Ni JD (2020) LncRNA TDRG1 promotes proliferation, invasion and epithelial-mesenchymal transformation of osteosarcoma through PI3K/AKT signal pathway. *Cancer Manag Res* **12**: 4531–4540. https://doi.org/10.2147/CMAR.S248964

Lamoureux F, Trichet V, Chipoy C, Blanchard F, Gouin F, Redini F (2007) Recent advances in the management of osteosarcoma and forthcoming therapeutic strategies. *Expert Rev Anticancer Ther* **7**: 169–181. https://doi.org/10.1586/14737140.7.2.169

Lin YH, Guo L, Yan F, Dou ZQ, Yu Q, Chen G (2020) Long non-coding RNA HOTAIRM1 promotes proliferation and inhibits apoptosis of glioma cells by regulating the miR-873-5p/ZEB2 axis. *Chin Med J (Engl)* **133**: 174–182. https://doi.org/10.1097/CM9.0000000000000615

Lindsey BA, Markel JE, Kleinerman ES (2017) Osteosarcoma Overview. *Rheumatol Ther* **4**: 25–43. https://doi.org/10.1007/s40744-016-0050-2

Liu Y, Wang Y, Yang H, Zhao L, Song R, Tan H, Wang L (2019) MicroRNA873 targets HOXA9 to inhibit the aggressive phenotype of osteosarcoma by deactivating the Wnt/betacatenin pathway. *Int J Oncol* **54**: 1809–1820. https://doi.org/10.3892/ijo.2019.4735

Ma D, Chang LY, Zhao S, Zhao JJ, Xiong YJ, Cao FY, Yuan L, Zhang Q, Wang XY, Geng ML, Zheng HY, Li O (2017) KLF5 promotes cervical cancer proliferation, migration and invasion in a manner partly dependent on TNFRSF11a expression. *Sci Rep* **7**: 15683. https://doi.org/10.1038/s41598-017-15979-1

Ma HZ, Wang J, Shi J, Zhang W, Zhou DS (2020) LncRNA LINC00467 contributes to osteosarcoma growth and metastasis through regulating HMGA1 by directly targeting miR-217. *Eur Rev Med Pharmacol Sci* **24**: 5933–5945. https://doi.org/10.26355/eurrev_202006_21486

Ma JB, Bai JY, Zhang HB, Jia J, Shi Q, Yang C, Wang X, He D, Guo P (2020) KLF5 inhibits STAT3 activity and tumor metastasis in prostate cancer by suppressing IGF1 transcription cooperatively with HDAC1. *Cell Death Dis* **11**: 466. https://doi.org/10.1038/s41419-020-2671-1

Misaghi A, Goldin A, Awad M, Kulidjian AA (2018) Osteosarcoma: a comprehensive review. *SICOT J* **4**: 12. https://doi.org/10.1051/sicotj/2017028

Pattison JM, Posternak V, Cole MD (2016) Transcription factor KLF5 binds a cyclin E1 polymorphic intronic enhancer to confer increased bladder cancer risk. *Mol Cancer Res* **14**: 1078–1086. https://doi.org/10.1158/1541-7786.MCR-16-0123

Ren Z, Liu X, Si Y, Yang D (2020) Long non-coding RNA DDX11-AS1 facilitates gastric cancer progression by regulating miR-873-5p/SPC18 axis. *Artif Cells Nanomed Biotechnol* **48**: 572–583. https://doi.org/10.1080/21691401.2020.1726937

Serra M, Hattinger CM (2017) The pharmacogenomics of osteosarcoma. *Pharmacogenomics J* **17**: 11–20. https://doi.org/10.1038/tpj.2016.45

Shang AQ, Wang WW, Yang YB, Gu CZ, Ji P, Chen C, Zeng BJ, Wu JL, Lu WY, Sun ZJ, Li D (2019) Knockdown of long noncoding RNA PVT1 suppresses cell proliferation and invasion of colorectal cancer via upregulation of microRNA-214-3p. *Am J Physiol Gastrointest Liver Physiol* **317**: G222–G232. https://doi.org/10.1152/ajpgi.00357.2018

Sun F, Yu Z, Wu B, Zhang H, Ruan J (2020) LINC00319 promotes osteosarcoma progression by regulating the miR-455-3p/NFIB axis. *J Gene Med* **22**: e3248. https://doi.org/10.1002/jgm.3248

Wang L, Jiang F, Ma F, Zhang B (2019) MiR-873-5p suppresses cell proliferation and epithelial-mesenchymal transition *via* directly targeting Jumonji domain-containing protein 8 through the NF-kappaB pathway in colorectal cancer. *J Cell Commun Signal* **13**: 549–560. https://doi.org/10.1007/s12079-019-00522-w

Wang L, Luo Y, Zheng Y, Zheng L, Lin W, Chen Z, Wu S, Chen J, Xie Y (2020) Long non-coding RNA LINC00426 contributes to doxorubicin resistance by sponging miR-4319 in osteosarcoma. *Biol Direct* **15**: 11. https://doi.org/10.1186/s13062-020-00265-4

Wang Z, Liu W, Wang C, Ai Z (2020) miR-873-5p Inhibits cell migration and invasion of papillary thyroid cancer *via* regulation of CXCL16. *Onco Targets Ther* **13**: 1037–1046. https://doi.org/10.2147/OTT.S213168

Yan L, Wu X, Yin X, Du F, Liu Y, Ding X (2018) LncRNA CCAT2 promoted osteosarcoma cell proliferation and invasion. *J Cell Mol Med* **22**: 2592–2599. https://doi.org/10.1111/jcmm.13518

Yao J, Lin J, He L, Huang J, Liu Q (2020) TNF-alpha/miR-155 axis induces the transformation of osteosarcoma cancer stem cells independent of TP53INP1. *Gene* **726**: 144224. https://doi.org/10.1016/j.gene.2019.144224

Zhang H, Lin J, Chen J, Gu W, Mao Y, Wang H, Zhang Y, Liu W (2020) DDX11-AS1 contributes to osteosarcoma progression via stabilizing DDX11. *Life Sci* **254**: 117392. https://doi.org/10.1016/j.lfs.2020.117392

Zhang W, Li JZ, Tai QY, Tang JJ, Huang YH, Gao SB (2020) LncRNA DANCR regulates osteosarcoma migration and invasion by targeting miR-149/MSI2 axis. *Eur Rev Med Pharmacol Sci* **24**: 6551–6560. https://doi.org/10.26355/eurrev_202006_21639

Zhao S, Xiong W, Xu K (2020) MiR-663a, regulated by lncRNA GAS5, contributes to osteosarcoma development through targeting MYL9. *Hum Exp Toxicol* **39**: 1607–1618. https://doi.org/10.1177/0960327120937330